Transport Activity of Human MRP3 Expressed in Sf9 Cells: Comparative Studies with Rat MRP3

Hidetaka Akita,[1] Hiroshi Suzuki,[1,3] Tomoko Hirohashi,[1] Hajime Takikawa,[2] and Yuichi Sugiyama[1]

Received July 23, 2001; accepted September 27, 2001

Purpose. Multidrug resistance-associated protein 3 (MRP3) was initially cloned as a hepatic transporter induced under cholestatic/hyperbilirubinemic conditions. In the present study, transport property of human MRP3 (hMRP3) was compared with that of rat MRP3 (rMRP3).

Methods. Adenosine 5′ triphosphate (ATP)-dependent uptake of several organic anions into the membrane vesicles isolated from the Sf9 cells expressing hMRP3 and rMRP3 was measured by rapid filtration technique.

Results. ATP-dependent uptake of glucuronide conjugates, glutathione conjugates, and [^{3}H]methotrexate (MTX) was stimulated by infection of cDNAs for hMRP3 and rMRP3. The mean (± SE) K_m values for the uptake of 17β estradiol 17β-D-glucuronide ([^{3}H]$E_2$17 βG) by hMRP3 and rMRP3 were 42.9 ± 4.3 μM and 33.4 ± 2.2 μM, respectively. Although the K_i values of glucuronides on the uptake of $E_2$17βG were similar in humans and rats, hMRP3 exhibited higher K_i values toward MTX. In addition, although glycocholate and taurolithocholate 3-sulfate (TLC-S) were transported by both hMRP3 and rMRP3, taurocholate was only transported to a significant degree by rMRP3. Moreover, the inhibitory effect of taurocholate and glycocholate on the transport of $E_2$17βG was much more potent in rMRP3 compared to hMRP3.

Conclusion. Collectively, the substrate specificity of hMRP3 resembles that of rMRP3 although differences were observed, particularly in bile acid transport.

KEY WORDS: ABC transporter; bile acids; MRP3; organic anion.

INTRODUCTION

Following the initial molecular cloning of multidrug resistance-associated protein (MRP) 1, an additional six MRP proteins referred to as MRP2–7 have been cloned from humans and experimental animals (1,2). Of all the MRP family proteins, the function of MRP1 and canalicular multispecific organic anion transporter (cMOAT)/MRP2 has been well characterized. Previous studies have shown that the substrate specificity of MRP1 and cMOAT/MRP2 are similar and that the substrates for these transporters include glutathione conjugates (such as leukotriene C_4 [LTC_4] and 2,4-dinitrophenyl-S-glutathione [DNP-SG]), glucuronide conjugates (such as 17β estradiol 17β-D-glucuronide [[^{3}H]$E_2$17 βG]), sulfated bile acids (such as taurolithocholate 3-sulfate [TLC-S]), and nonconjugated organic anions (such as methotrexate [MTX]) (3–7).

Previously, we have cloned rat MRP3 (rMRP3) as an inducible transporter under cholestatic/hyperbilirubinemic conditions; rMRP3 was induced in Eisai hyperbilirubinemic rats whose cMOAT/MRP2 function is hereditarily defective and in SD rats subjected to common bile duct ligation (8–10). Moreover, we found that the expression of human MRP3 (hMRP3) was induced by phenobarbital in HepG2 cells in culture (11). Based on immunohistochemical studies, König *et al.* (12) showed that hMRP3 is expressed on the basolateral membrane of hepatocytes and is overexpressed in patients with Dubin-Johnson syndrome, suggesting that hMRP3 is also induced under hyperbilirubinemic conditions. The basolateral expression of hMRP3 on hepatocytes and cholangiocytes was also reported by Kool *et al.* (13). It is possible that MRP3 functions as efflux transporter from hepatocytes to circulating blood to switch the excretion route for organic anions from bile to urine under the pathologic conditions. Indeed, using membrane vesicles prepared from LLC-PK1 cells and HeLa cells transfected with rMRP3 cDNA, we have shown that MRP3 transports some organic anions, including glucuronide conjugates (e.g., $E_2$17βG) and MTX (14). More recently, it has been demonstrated that rMRP3 transports several kinds of bile acids (15). To examine the function of hMRP3, Kool *et al.* (13) infected Madin-Darby canine kidney (MDCK) II cells with its cDNA. They found that the cDNA product is expressed on the basolateral membrane and is responsible for the basal efflux of DNP-SG, after preloading the cells with its precursor (13). The hMRP3-expressing MDCK II cells also acquired resistance to anticancer agents (13,16). In the present study, we prepared membrane vesicle from Sf9 cells infected with recombinant baculovirus containing hMRP3 and rMRP3 cDNA to characterize the species differences for the function of MRP3.

MATERIALS AND METHODS

Materials

[^{3}H]$E_2$17βG (44 Ci/mmol), [^{3}H]taurocholate (TC; 2.0 Ci/mmol) and [^{3}H]LTC_4 (146.0 Ci/mmol) were purchased from NEN Life Science Products (Boston, MA). [^{14}C]Glycocholate (GC; 55 mCi/mmol) and [^{3}H]MTX (30 Ci/mmol) were purchased from American Radiolabeled Chemicals, Inc (Bowing, MO). Unlabeled and ^{3}H-labeled DNP-SG (22.5 Ci/mmol) were synthesized enzymatically using [glycine-2-^{3}H]glutathione (NEN Life Science Products) and 1-chloro-2,4-dinitrobenzene and glutathione S-transferase (Sigma Chemical Co., St.Louis, MO) as described previously (17). [^{14}C] 6-Hydroxy-5,7-dimethyl-2-methylamino-4-(3-pyridylmethyl) benzothiazole (E3040) glucuronide (84.5 mCi/mmol) and unlabeled E3040 glucuronide and sulfate were prepared from E3040 (supplied by Eisai Co., Ltd., Tsukuba,

[1] Graduate School of Pharmaceutical Sciences, The University of Tokyo, Hongo, Bunkyo-ku, Tokyo 113-0033, Japan.

[2] Department of Medicine, Teikyo University School of Medicine, Kaga, Itabashi-Ku, Tokyo 173-0003, Japan.

[3] To whom correspondence should be addressed. (e-mail: Seizai.Suzuki@nifty.ne.jp)

ABBREVIATIONS: AMP, adenosine monophosphate; ATP, adenosine 5′ triphosphate; DNP-SG, 2,4-dinitrophenyl-S-glutathione; GC, glycocholate; GFP, green fluorescent protein; hMRP, human multidrug resistance-associated protein; LTC, leukotriene C_4; MDCK, Madin-Darby canine kidney; MRP, multidrug resistance-associated protein; MTX, methotrexate; rMRP, rat multidrug resistance-associated protein; TC, taurocholate; TLC-S, taurolithocholate 3-sulfate.

0724-8741/02/0100-0034/0 © 2002 Plenum Publishing Corporation

Japan) as described previously (18). [^{3}H]TLC-S was synthesized from lithocholate-3-sulfate using [2-^{3}H]taurine (30.3 Ci/mmol) (NEN Life Science Products) as described previously (19). 4-Methyl-umbelliferone (4-MU) glucuronide, 4-MU sulfate, LTC_4, MTX, estrone sulfate, TC, GC, and TLC-S were purchased from Sigma Chemical Co (St. Louis, MO).

Preparation of Membrane Vesicles from Sf9 Cells Expressing hMRP3 and rMRP3

The Bac-to-Bac system (Life Technologies Inc., Gaithersburg, MD) was used to establish the recombinant baculovirus. *Xba I-Kpn I* fragment containing the full length of hMRP3 (11) and *BamH I-Kpn I* fragment containing the full length of rMRP3 (8) were inserted into pFastBact (Life Technologies Inc.) downstream of the polyhedrin promoter. As a negative control, green fluorescence protein (GFP), a cytosolic protein was used to allow monitoring of the infection efficiency. Sf9 cells were infected with the virus at 27°C for 72 h. For the preparation of membrane vesicle, Sf9 cells were scraped from culture dishes, centrifuged at 1,500 × *g,* and suspended in hypotonic buffer (1 mM Tris-HCl, pH 7.0) and gently stirred for 1.5 h. Then, the solution was centrifuged at 10,000 × *g* and diluted with isotonic buffer (10 mM Tris-HCl, pH 7.4; and 250 mM sucrose). Disrupted cells were homogenized with a glass/glass homogenizer and applied to a 38% sucrose solution (Tris/Hepes, pH 7.4). After centrifugation at 280,000 × *g* for 45 min, the turbid layer was recovered and centrifuged at 100,000 × *g*. The pellet was diluted with the transport buffer (10 mM Tris, 250 mM sucrose, and 10 mM $MgCl_2$, pH 7.4) and passed through a 25-gauge needle. These membrane vesicle preparations were rapidly frozen in liquid N_2 and were kept at –80 ^{0}C until required.

Preparation of Antibody

The polyclonal antibodies to hMRP3 and rMRP3 were obtained by immunizing rabbits with a maltose-binding protein fusion protein containing the 147 and 136 amino acids corresponding to 836-983 and 838-973 of the deduced amino acid sequence, respectively. The pMAL-c2 expression vector (New England Biolabs, Inc., Beverly, MA) was used for the expression of the fusion protein. After purification using amylose resin, rabbits were immunized with 250 μg fusion protein mixed with Freund's complete adjuvant (Sigma Chemical Co.).

Western Blot Analysis

Membrane vesicles (25 μg) prepared as described above were solubilized in sample buffer consisting of 2% SDS, 30% glycerol, and 0.01% bromophenol blue (pH 6.8). The suspension was subjected to electrophoresis on 8.5% polyacrylamide gel with 0.1% SDS and electrotransferred to a polyvinylidene difluoride membrane (Millipore, Bedford, MA). The filter was blocked with Tris-buffer/saline solution containing 0.05% Tween 20% and 5% bovine serum albumin for 1 h at room temperature and was probed overnight at 4°C with polyclonal antibody (dilution 1:1000) that was prepared as described above. Antibody was visualized with [^{125}I] anti-rabbit antibody (Amersham Corp., Buckinghamshire, England), followed by exposure to Fuji imaging plates (Fuji Photo Film Co., Ltd., Kanagawa, Japan) for 3 h at room temperature, and was analyzed with an imaging analyzer (BSA 2000, Fuji Photo Film Co., Ltd.).

Transport Studies with Sf9-Membrane Vesicles

Transport studies were performed using the rapid filtration technique reported previously (20). The transport medium contained the isotopically labeled ligand, 5 mM adenosine 5′ triphosphate (ATP) or 5 mM adenosine monophosphate (AMP), and an ATP-regenerating system (10 mM creatine phosphate, 10 mM $MgCl_2 \cdot 6H_2O$, and 100 μg/ml creatine phosphokinase, pH 7.4). A 16-μl aliquot of transport medium was mixed rapidly with 4 μl vesicle suspension (5–10 μg protein). In the inhibition study, several compounds were dissolved in transport buffer at the indicated concentrations.

The transport reaction was stopped by the addition of 1 ml ice-cold buffer containing 250 mM sucrose, 0.1 M NaCl, and 10 mM Tris-HCl (pH 7.4). The stopped reaction mixture was filtered through a 0.45-μm HA filter (Millipore Corp., Bedford, MA) and then was washed twice with a 10-ml stop solution. The radioactivity retained on the filter and in the reaction mixture was measured in a liquid scintillation counter (LS 6000SE, Beckman Instruments, Fullerton, CA) following the addition of scintillation cocktail (Clear-sol I, Nacalai Tesque, Tokyo, Japan). Radioactivity retained on the filter was the same when a 0.22-μm HA filter was used for the uptake study of $E_2$17βG, suggesting that the loss of membrane vesicles by filtration through the 0.45-μm HA filter is negligible (data not shown). Ligand uptake activity is given by normalizing the amount associated with the membrane vesicles (pmol/mg protein) by the ligand concentration in the medium (μM = pmol/μl).

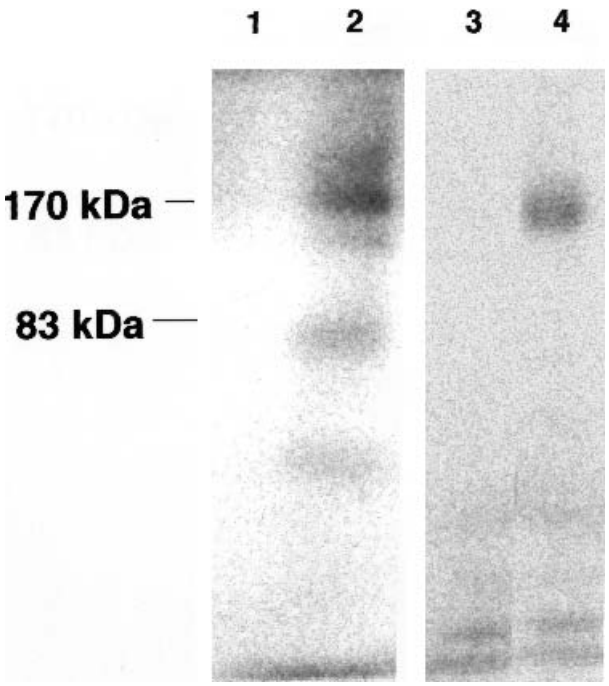

Fig. 1. Western blot analysis of hMRP3 and rMRP3 proteins in membrane vesicles isolated from infected Sf9 cells. Membrane vesicles (25 μg) prepared from hMRP3-, rMRP3-, and GFP-expressing Sf9 cells (25 μg) were separated on an 8.5% polyacrylamide gel containing 0.1 % SDS. The proteins transferred to the polyvinylidene difluoride membrane by electroblotting were detected by polyclonal anti-hMRP3 (lanes 1 and 2) and anti-rMRP3 (lanes 3 and 4) antiserum. Lane 1 and 3, GFP expressing Sf9; lane 2, hMRP3 expressing Sf9 (25 μg); lane 4, rMRP3 expressing Sf9 (25 μg).

The ATP-dependent uptake was determined by subtracting the uptake in the absence of ATP from that in the presence of ATP. The kinetic parameters were estimated as described previously (20).

RESULTS

Uptake of Organic Anions into Membrane Vesicles

The expression of human and rat MRP3 in infected cells was detected by Western blot analysis (Fig. 1). The antibodies recognized bands of approximately 170 kDa for both hMRP3 and rMRP3 (Fig. 1), which is shorter than that observed in mammalian cells presumably due to the lower degree of glycosylation. In addition, no bands were observed in negative control cell lines, which express only GFP, a cytosolic protein.

Time-profiles for the uptake of conjugates ([^{3}H]DNP-SG, [^{3}H]LTC$_4$, [^{3}H]E$_2$17βG, and [^{14}C]E3040-glu) by membrane vesicles from Sf9 cells are shown in Fig. 2. ATP-dependent uptake of glucuronide-conjugates ([^{3}H]E$_2$17βG and [^{14}C]E3040-glu) was stimulated in hMRP3- and rMRP3-expressing Sf9 cells (Fig. 2). Although significant ATP-dependent uptake of glutathione conjugates ([^{3}H]DNP-SG and [^{3}H]LTC$_4$) was observed even in the control membrane vesicles, the expression of hMRP3 and rMRP3 increased the uptake (Fig. 2), suggesting that these glutathione conjugates are also transported by both hMRP3 and rMRP3.

A kinetics analysis revealed that the ATP-dependent uptake of [^{3}H]E$_2$17 βG into membrane vesicles from hMRP3- and rMRP3-infected Sf9 cells can be described by a single saturable component with K_m = 42.9 ± 4.3 μM and V_{max} = 553 ± 29 pmol/min/mg protein for the former, and K_m = 33.4 ± 2.2 μM and V_{max} = 1.47 ± 0.08 nmol/min/mg protein for the latter (Fig. 3). ATP-dependent uptake of DNP-SG and LTC$_4$ via hMRP3 and rMRP3 was not enough to demonstrate the kinetics analysis for these compounds.

Figure 4 shows the time-profile for the uptake of [^{3}H]MTX into membrane vesicles expressing human and rat MRP3. ATP-dependent uptake of [^{3}H]MTX was stimulated by infection of hMRP3 and rMRP3 cDNAs. In addition, ATP-dependent uptake of [^{3}H]MTX was inhibited by E$_2$17βG and E3040-glu in a concentration-dependent manner (Fig. 4). Moreover, the uptake of [^{3}H]MTX was inhibited by 1 mM unlabeled MTX for rMRP3, whereas only slight inhibition was observed for hMRP3 (Fig. 4).

Figure 5 shows the time-profiles for uptake of monovalent bile acids ([^{3}H]TC and [^{3}H]GC) and sulfate-conjugated bile acid ([^{3}H]TLC-S) into membrane vesicles isolated from hMRP3- and rMRP3-expressing Sf9 cells. For rMRP3, the uptake of [^{3}H]TC and [^{3}H]GC was stimulated by baculovirus infection. In contrast, no ATP-dependent uptake of [^{3}H]TC was detected for hMRP3, although that of [^{3}H]GC was significant (Fig. 5). Moreover, the ATP-dependent uptake of [^{3}H]TLC-S was stimulated to 236% and 197% of that of the GFP control by the expression of hMRP3 and rMRP3, sug-

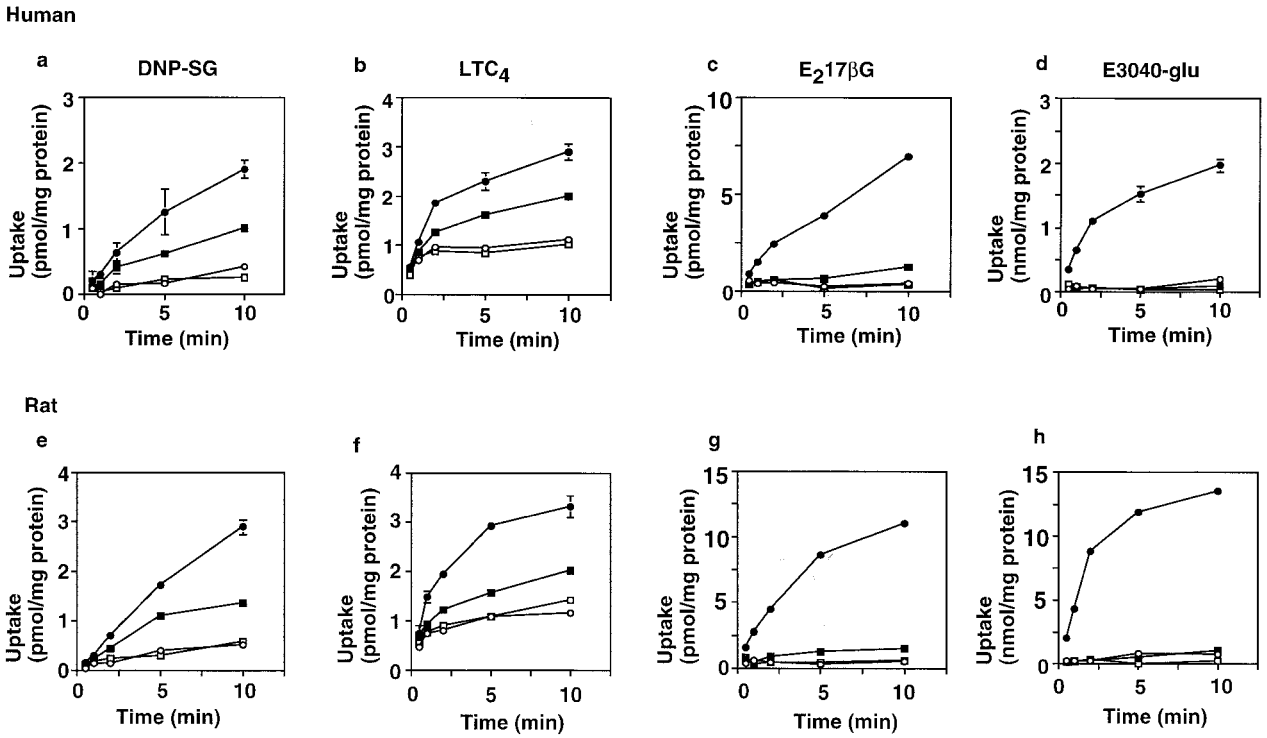

Fig. 2. Time-profiles for the uptake of conjugated compounds. Membrane vesicles (10 μg protein) from human (upper) and rat (lower) MRP3-expressing (circles) or GFP-expressing (squares) Sf9 cells were incubated at 37°C with 5 mM ATP (closed symbols) or AMP (opened symbols) and ATP-regenerating system in medium containing 100 nM [^{3}H]DNP-SG (panels a and e), 5 nM [^{3}H]LTC$_4$ (panels b and f), 50 nM [^{3}H]E$_2$17 βG (panels c and g), and 10 μM [^{14}C]E3040-glu (panels d and h). Uptake amount (pmol/mg protein) was normalized by the ligand concentration (pmol/μl). Each point and vertical bar represent the mean ± SE of triplicate determinations (closed symbols) or the mean of two determinations (open symbols).

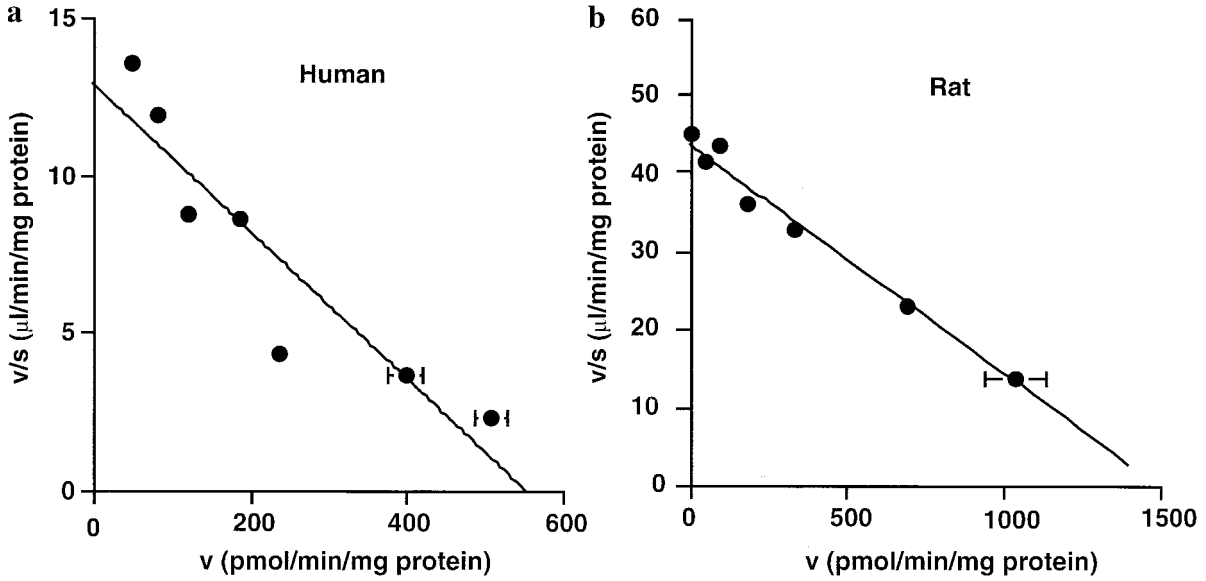

Fig. 3. Eadie-Hofstee plot for the uptake of $E_2$17 βG by membrane vesicles. Membrane vesicles isolated from hMRP3-expressing (a) and rMRP3-expressing (b) Sf9 cells were incubated at 37°C for 2 min with 5 mM ATP or AMP and ATP-regenerating system in medium containing 100 nM [^{3}H]$E_2$17 βG and different concentration of $E_2$17 βG (2 – 100 μM). The ATP-dependent uptake was obtained by subtracting the values in the absence of 5 mM ATP from those in the presence of ATP. Each point and vertical/horizontal bar represent the mean ± SE of triplicate determinations (closed symbols).

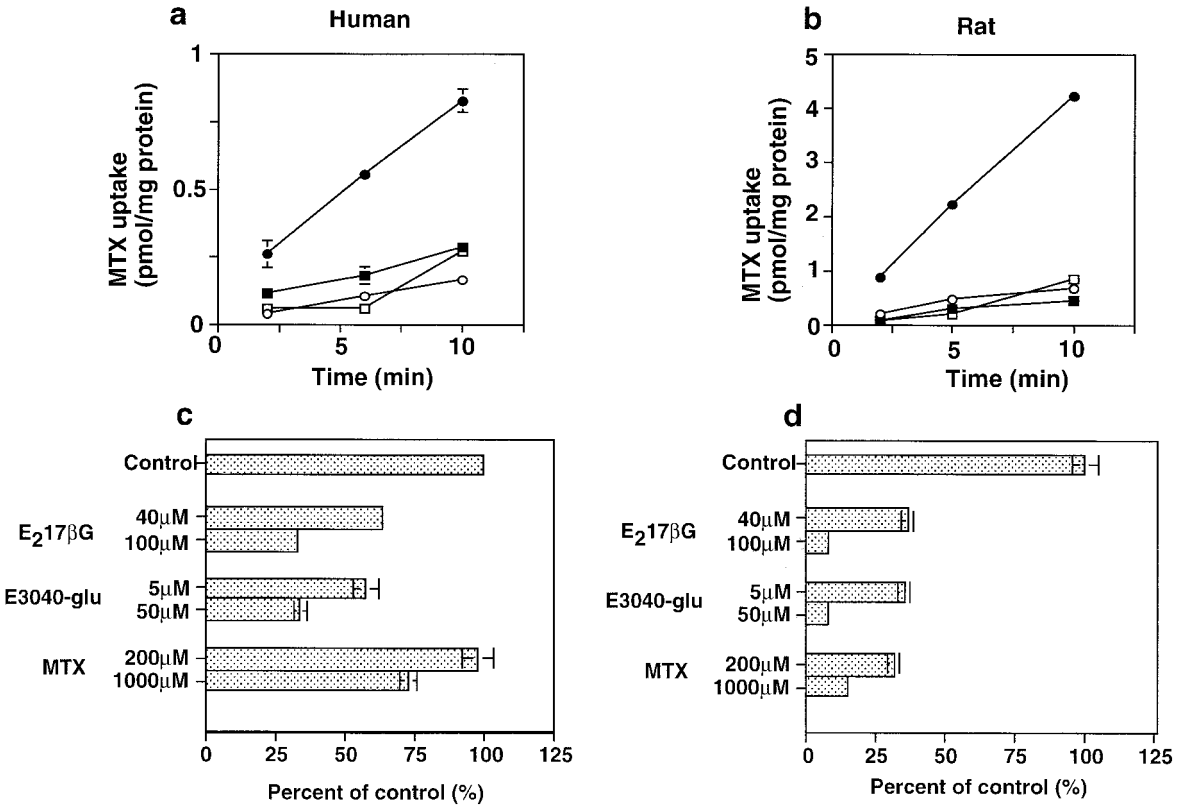

Fig. 4. Time-profiles for the uptake of [^{3}H] MTX (a and b) and inhibitory effect of several organic anions for the uptake of [^{3}H] MTX (panel c and d). Membrane vesicles (10 μg protein) from human (a) and rat (b) MRP3-expressing (circle) or GFP-expressing (square) Sf9 cells were incubated at 37°C with 5 mM ATP (closed symbols) or AMP (open symbols) and ATP-regenerating system in medium containing 120 nM [^{3}H]MTX. Uptake amount (pmol/mg protein) was normalized by the ligand concentration (pmol/μl). Each point and vertical bar represent the mean ± SE of triplicate determinations (closed symbols) or the mean of two determinations (open symbols). ATP-dependent uptake of [^{3}H] MTX for 10 min via hMRP3 (c) and rMRP3 (d) was calculated by subtracting values in the absence of 5 mM ATP from those in the absence of ATP. Transport was expressed as percent of control uptake. Each bar and horizontal bar represent the mean ± SE of triplicate determinations.

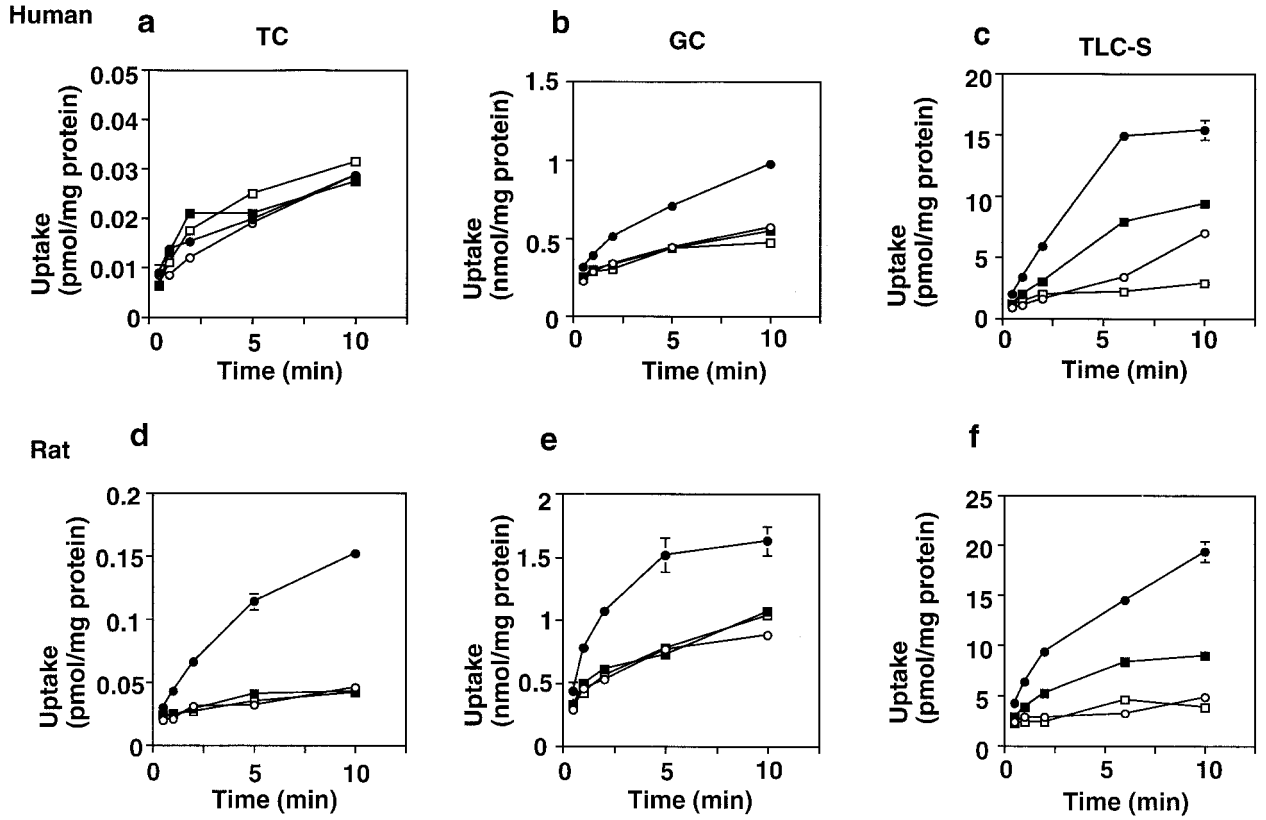

Fig. 5. Time-profiles for the uptake of bile acids. Membrane vesicles (10 μg protein) from human (upper) and rat (below) MRP3-expressing (circle) or GFP-expressing (square) Sf9 cells were incubated at 37°C with 5 mM ATP (closed symbols) or AMP (open symbols) and ATP-regenerating system in medium containing 1.2 nM [^{3}H]TC (a and d), 25 μM [^{14}C] GC (b and e), and 25 nM [^{3}H]TLC-S (c and f). Uptake amount (pmol/mg protein) was normalized by the ligand concentration (pmol/μl). Each point and vertical bar represent the mean ± SE of triplicate determinations (closed symbols) or the mean of two determinations (open symbols)

gesting that hMRP3 and rMRP3 accept sulfate-conjugated bile acids along with the monovalent bile acids (Fig. 5).

To compare the transport activity between hMRP3 and rMRP3, the relationship between the values for the initial ATP-dependent uptake of a series of organic anions was examined in the two mammalian species. The values for the enhanced ATP-dependent uptake rate by hMRP3 and rMRP3 expression to that of GFP control calculated from Figs. 2, 4, and 5 were plotted in Fig. 6. The initial ATP-dependent uptake rate for several compounds was well correlated between hMRP3 and rMRP3 ($r = 0.99$), suggesting that substrate specificity of hMRP3 was similar to that of rMRP3 (Fig. 6). The only exception involved TC; rMRP3 accepted TC in preference to hMRP3 (Fig. 6).

Effect of Organic Anions on ATP-Dependent Uptake of [^{3}H]$E_2$17 βG

Table 1 shows the effect of organic anions on the hMRP3-mediated uptake of [^{3}H]$E_2$17 βG. K_i values for hMRP3 estimated from this study and those for rMRP3 calculated from Hirohashi *et al.* (14) were also included in Table 1. Glucuronide conjugates (E3040-glu and 4-MU glucuronide) significantly inhibited the uptake of [^{3}H]$E_2$17 βG via hMRP3 and rMRP3 with comparable K_i values of 5.6 ± 1.0 μM and 105 ± 21 μM, and 2.6 ± 0.2 μM and 77 ± 12 μM, respectively (Table 1). Moreover, the inhibitory effect of MTX was much less potent for hMRP3 than that for rMRP3 (Table 1). K_i values of MTX against hMRP3 and rMRP3 were >1 mM and 90.0 ± 23.7 μM, respectively (Table 1). In addition, a stimulatory effect by sulfate conjugates (E3040 sulfate and 4-MU sulfate) was observed (see Fig. 8). The inhibitory effect of TC and GC on the uptake of [^{3}H]$E_2$17 βG is shown in Fig. 7. The K_i values of TC and GC on hMRP3 function (538 ± 41 μM and 847 ± 256 μM, respectively) were much larger than those on rMRP3 (74.2 ± 17.6 μM and 46.8 ± 7.0 μM, respectively) (Fig. 7).

DISCUSSION

In the present study, we compared the substrate specificity between hMRP3 and rMRP3 using membrane vesicles from Sf9 cells infected with baculoviruses containing these cDNAs. Western blot analysis indicated the expression of both hMRP3 and rMRP3 at approximately 170 kDa (Fig. 1), which was similar to the reported values for MRP family members (3,4,6).

We found a nice correlation in the initial velocity for the uptake of a series of organic anions between hMRP3 and rMRP3, with monovalent bile acids being the only exception (Fig. 6). This suggests that transport ability for several organic anions is similar between hMRP3 and rMRP3. Indeed, both hMRP3 and rMRP3 can accept both glucuronide and glutathione conjugates (Fig. 2) (14). Moreover, like rMRP3, the

Table I. Effects of Compounds on the ATP-Dependent Uptake of [^{3}H]$E_2$17βG by Membrane Vesicles from Human MRP3-Expressing Sf9 Cells[a]

Inhibitor	Concentration (μM)	% Control	Ki	
			Human	Rat
Control		100		
E3040 glucuronide	2	69.5 ± 4.8		
	10	35.3 ± 4.7		
	50	18.1 ± 1.3	5.6 ± 1.0 μM	2.6 ± 0.2 μM
	100	10.8 ± 1.8		
	500	2.2 ± 1.0		
4-Methylumbelliferone glucuronide	2	83.9 ± 5.8		
	10	82.5 ± 1.8		
	30	68.2 ± 5.5	105 ± 21 μM	77.0 ± 11 μM
	125	35.1 ± 0.9		
	500	23.0 ± 2.2		
MTX	10	80.4 ± 6.8		
	50	78.3 ± 0.9		
	200	70.0 ± 3.7	1.2 ± 0.2 mM	90.0 ± 23 μM
	500	63.3 ± 3.8		
	1000	64.2 ± 3.5		
DNP-SG	5	82.2 ± 2.7		
	20	83.0 ± 5.9		
	50	76.0 ± 1.9	337 ± 41 μM	83.8 ± 2.7 μM
	150	71.5 ± 2.6		
	500	42.8 ± 2.4		
	1000	24.1 ± 1.4		
LTC_4	0.1	92.8 ± 5.4		
	0.5	93.9 ± 4.2	>10 μM	~2.5 μM
	2.5	99.3 ± 2.7		
	10	86.4 ± 5.8		

[a] Inhibitory effect is given as the mean ± SE whereas ki values are given as the mean ± SD.

transport activity of hMRP3 for $E_2$17βG was much higher than that for DNP-SG (Fig. 6), which is different from that of human MRP2 (21). Our data are also consistent with the recent study showing that the transport activity of hMRP3 for DNP-SG and MTX, defined as V_{max}/K_m, was lower than that for $E_2$17βG (22). The fact that hMRP3 transports DNP-SG (Fig. 2) is consistent with the previous observations (13), in which there was accelerated export of DNP-SG from hMRP3-transfected MDCK II cells after preloading the cells with precursor (1-chloro-2,4-dinitrobenzene). In addition, hMRP3-transfected mammalian cells acquired resistance to MTX (13,16). Their results are also consistent with our present results showing that hMRP3 can also transport MTX (Fig. 4). Furthermore, the kinetics parameters for the transport of organic anions by hMRP3 were similar to that by rMRP3. For example, K_m values for $E_2$17βG were similar in the two animal species (42.9 ± 4.3 and 33.4 ± 2.2 μM for hMRP3 and rMRP3, respectively; Fig. 3). The K_m value for $E_2$17βG via hMRP3 was also comparable with that reported recently (22). The inhibitory effect of glucuronide conjugates was similar for both hMRP3 and rMRP3; the K_i values of E3040-glu and 4-MU glucuronide were less than 5 μM and approximately 50 μM, respectively, for both hMRP3 and rMRP3 (Table 1) (14). These results are consistent with the findings in the inhibition studies for the uptake of [^{3}H]MTX (Fig. 4). The ATP-dependent transport of [^{3}H]MTX by hMRP3 and rMRP3 was inhibited by 40 μM $E_2$17βG and 5 μM E3040-glu to 40–60% of the control, which is accounted for by considering the K_m

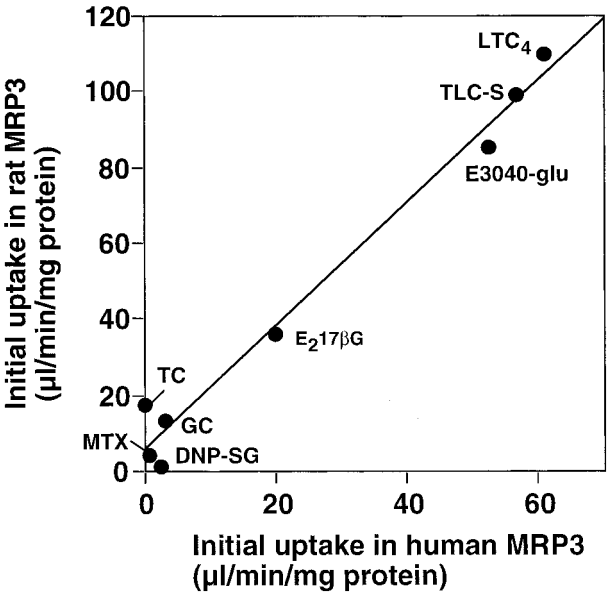

Fig. 6. Comparison of the initial ATP-dependent uptake of several organic anions by membrane vesicles prepared from hMRP3- and rMRP3-expressing Sf9 cells. ATP-dependent uptake rate (pmol/min/mg protein) was normalized by the medium concentration (pmol/μl). Mean values for ATP-dependent uptake in hMRP3 and rMRP3 for 2 min were cited from Figs. 2, 4, and 5.

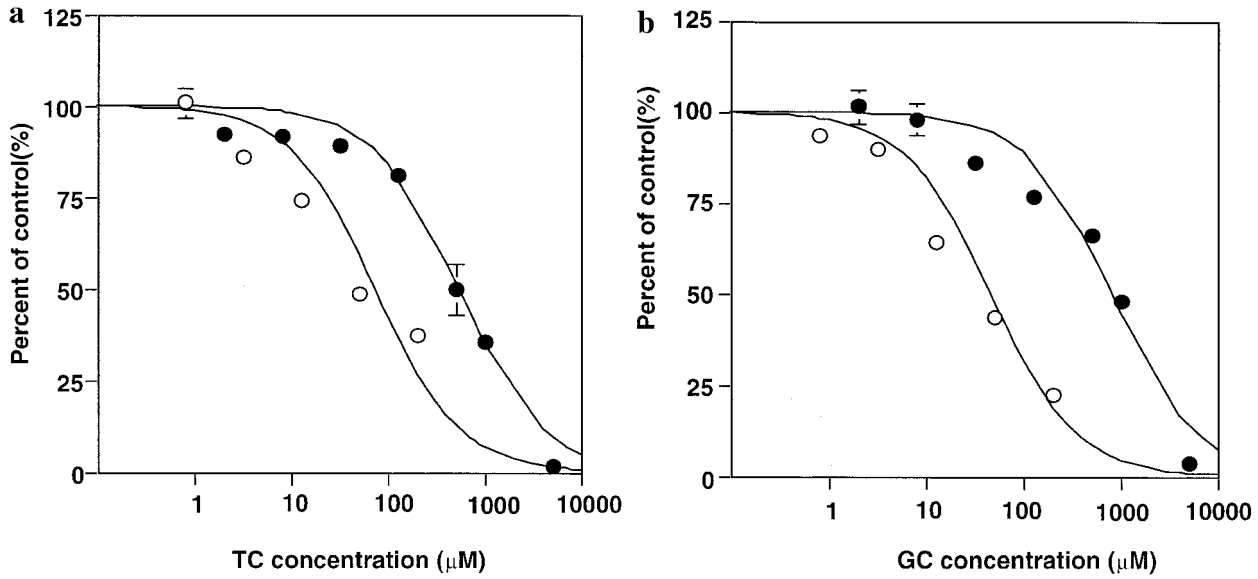

Fig. 7. Effect of TC and GC on the ATP-dependent uptake of [^{3}H]$E_2$17βG by membrane vesicles isolated from hMRP3- and rMRP3-expressing Sf9 cells. Membrane vesicles isolated from human (closed circle) and rat (open circle) MRP3-expressing Sf9 cells were incubated at 37°C for 2 min, with 5 mM ATP or AMP and ATP-regenerating system in medium containing 50 nM [^{3}H] $E_2$17 βG and different concentrations of TC (a) and GC (b) at the indicated concentrations. The ATP-dependent uptake was obtained by subtracting the values in the absence of ATP from those in the presence of ATP. Transport was expressed as percentage of the control uptake. Each point and vertical bar represent the mean ± SE of three different experiments

and K_i values of these glucuronide conjugates (Fig.4). In the present study, it was demonstrated that sulfate conjugates, such as E3040 sulfate and 4-MU sulfate, stimulated the hMRP3-mediated transport of $E_2$17βG (Fig. 8). These results

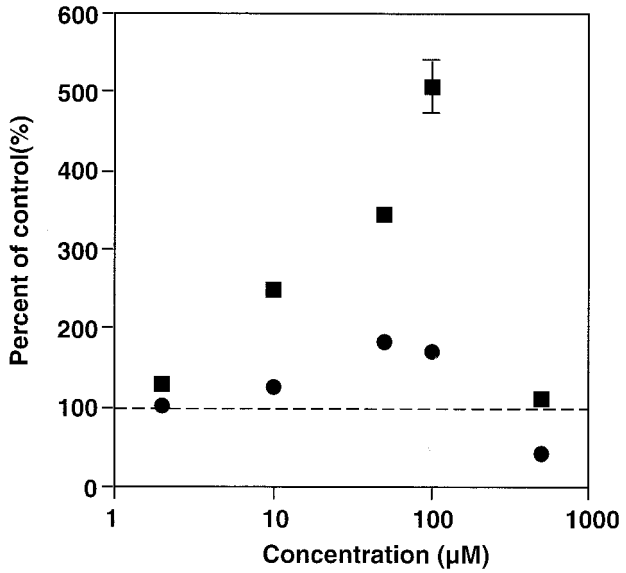

Fig. 8. Effect of E3040 sulfate and 4-MU sulfate on the ATP-dependent uptake of [^{3}H]$E_2$17βG by membrane vesicles isolated from hMRP3-expressing Sf9 cells. Membrane vesicles isolated from hMRP3-expressing Sf9 cells were incubated at 37°C for 2 min, with 5 mM ATP or AMP and ATP-regenerating system in medium containing 50 nM [^{3}H] $E_2$17 βG, and different concentrations of E3040 sulfate (circle) and 4-MU sulfate (square) at the indicated concentrations. The ATP-dependent uptake was obtained by subtracting the values in the absence of ATP from those in the presence of ATP. Transport was expressed as percentage of the control uptake. Each point and vertical bar represent the mean ± SE of three different experiments

are consistent with previous observations for mammalian MRP family proteins. We have indicated that E3040 sulfate and 4-MU sulfate stimulate the uptake of DNP-SG and $E_2$17βG into isolated rat canalicular membrane vesicles expressing MRP2 and into membrane vesicles from rMRP3-expressing LLC-PK_1 cells, respectively (14,20). In addition, Bakos *et al.* (23) recently reported the stimulatory effect of indomethacin, sulfinpyrazone, and benzylpenicillin on MRP1- and MRP2-mediated transport of N-ethylmaleimide-glutathione. Although the mechanism for these stimulation remains to be clarified, it is possible that MRP family proteins may have an allosteric site as has been suggested for MDR1 (24).

A marked difference was observed between hMRP3 and rMRP3 in terms of the kinetic parameters for the transport of MTX and bile acids. The affinity of hMRP3 for MTX (Ki = 1.2 mM; Table 1) was much lower than that of rMRP3 (Ki = 90 μM; Table 1). This is in good agreement with the finding that the ATP-dependent uptake of [^{3}H]MTX was reduced by 70% by 200 μM unlabeled MTX in rMRP3 (Fig. 4), whereas only a 30% reduction was observed in hMRP3 even in the presence of 1 mM MTX (Fig. 4). In the same manner, the inhibitory effect of TC and GC on rMRP3 was approximately 10–20 times more potent than that on hMRP3 (Fig. 7).

Moreover, TC was significantly transported by rMRP3, but not by hMRP3 (Fig. 5). For hMRP3, GC was a better substrate than TC, whereas TC was preferentially transported by rMRP3 rather than GC (Fig. 5). Similar to hMRP3, human ileal Na^+-bile acid cotransporter has higher transport activity for GC than that for TC (25). It has been reported that approximately 70% of bile acids are present as glycine conjugates in humans, whereas >90% are present as taurine conjugates in rats under physiologic conditions (26,27). Considering this species difference in endogenous bile acid composition, preferential transport of GC compared with TC

by human transporters may have some physiologic significance.

Collectively, these results indicate that the substrate specificity of hMRP3 resembles that of rMRP3, although some major differences were observed, particularly in the transport of bile acids and inhibitory effect of MTX and monovalent bile acids.

ACKNOWLEDGMENT

This work was supported by a Grant-in-Aid for Scientific Research on Priority Areas "ABC proteins" (No. 10044243) from the Ministry of Education, Science, and Culture of Japan.

REFERENCES

1. M. Kool, M. de Haas, G. L. Scheffer, R. J. Scheper, M. J. van Eijk, J. A. Juijn, F. Baas, and P. Borst. Analysis of expression of cMOAT (MRP2), MRP3, MRP4, and MRP5, homologues of the multidrug resistance-associated protein gene (MRP1), in human cancer cell lines. *Cancer Res.* **57**:3537–3547 (1997).
2. P. Borst. Multidrug resistant proteins. *Semin. Cancer Biol.* **8**:131–134 (1997).
3. R. G. Deeley and S. P. Cole. Function, evolution and structure of multidrug resistance protein (MRP). *Semin. Cancer Biol.* **8**:193–204 (1997).
4. D. Keppler and J. König. Hepatic canalicular membrane 5: expression and localization of the conjugate export pump encoded by the MRP2 (cMRP/cMOAT) gene in liver. *FASEB J.* **11**:509–516 (1997).
5. R. P. Oude Elferink, D. K. Meijer, F. Kuipers, P. L. Jansen, A. K. Groen, and G. M. Groothuis. Hepatobiliary secretion of organic compounds: molecular mechanisms of membrane transport. *Biochim. Biophys. Acta* **1241**:215–268 (1995).
6. M. Müller and P. L. Jansen. Molecular aspects of hepatobiliary transport. *Am. J. Physiol*. **272**:G1285–G1303 (1997).
7. H. Suzuki and Y. Sugiyama. Excretion of GSSG and glutathione conjugates mediated by MRP1 and cMOAT/MRP2. *Semin. Liver Dis.* **18**:359–376 (1998).
8. T. Hirohashi, H. Suzuki, K. Ito, K. Ogawa, K. Kume, T. Shimizu, and Y. Sugiyama. Hepatic expression of multidrug resistance-associated protein-like proteins maintained in eisai hyperbilirubinemic rats. *Mol. Pharmacol.* **53**:1068–1075 (1998).
9. K. Ogawa, H. Suzuki, T. Hirohashi, T. Ishikawa, P. J. Meier, K. Hirose, T. Akizawa, M. Yoshioka, and Y. Sugiyama. Characterization of inducible nature of MRP3 in rat liver. *Am. J. Physiol.* **278**:G438–G446 (2000).
10. C. J. Soroka, J. M. Lee, F. Azzaroli, and J. L. Boyer. Cellular localization and up-regulation of multidrug resistance-associated protein 3 in hepatocytes and cholangiocytes during obstructive cholestasis in rat liver. *Hepatology* **33**:783–791 (2001).
11. Y. Kiuchi, H. Suzuki, T. Hirohashi, C. A. Tyson, and Y. Sugiyama. cDNA cloning and inducible expression of human multidrug resistance associated protein 3 (MRP3). *FEBS Lett.* **433**: 149–152 (1998).
12. J. König, D. Rost, Y. Cui, and D. Keppler. Characterization of the human multidrug resistance protein isoform MRP3 localized to the basolateral hepatocyte membrane. *Hepatology* **29**:1156–1163 (1999).
13. M. Kool, M. van der Linden, M. de Haas, G. L. Scheffer, J. M. de Vree, A. J. Smith, G. Jansen, G. J. Peters, N. Ponne, R. J. Scheper, R. P. Elferink, F. Baas, and P. Borst. MRP3, an organic anion transporter able to transport anti-cancer drugs. *Proc. Natl. Acad. Sci. USA* **96**:6914–6919 (1999).
14. T. Hirohashi, H. Suzuki, and Y. Sugiyama. Characterization of the transport properties of cloned rat multidrug resistance-associated protein 3 (MRP3). *J. Biol. Chem.* **274**:15181–15185 (1999).
15. T. Hirohashi, H. Suzuki, H. Takikawa, and Y. Sugiyama. ATP-dependent transport of bile salts by rat multidrug resistance-associated protein 3 (Mrp3). *J. Biol. Chem.* **275**:2905–2910 (2000).
16. H. Zeng, L. J. Bain, M. G. Belinsky, and G. D. Kruh. Expression of multidrug resistance protein-3 (multispecific organic anion transporter-D) in human embryonic kidney 293 cells confers resistance to anticancer agents. *Cancer Res.* **59**:5964–5967 (1999).
17. K. Kobayashi, Y. Sogame, H. Hara, and K. Hayashi. Mechanism of glutathione S-conjugate transport in canalicular and basolateral rat liver plasma membranes. *J. Biol. Chem.* **265**:7737–7741 (1990).
18. O. Takenaka, T. Horie, H. Suzuki, and Y. Sugiyama. Different biliary excretion systems for glucuronide and sulfate of a model compound; study using Eisai hyperbilirubinemic rats. *J. Pharmacol. Exp. Ther.* **274**:1362–1369 (1995).
19. J. Zhang, W. J. Griffiths, and J. Sjövall. The synthesis of btaurine-conjugated bile acids and bile acid sulfates labeled with 1^{4C} or 3^{H} in the taurine moiety. *J. Labelled Compd. Radiopharm.* **39:**154–164 (1997).
20. K. Niinuma, O. Takenaka, T. Horie, K. Kobayashi, Y. Kato, H. Suzuki, and Y. Sugiyama. Kinetic analysis of the primary active transport of conjugated metabolites across the bile canalicular membrane: comparative study of S-(2,4-dinitrophenyl)-glutathione and 6-hydroxy-5,7-dimethyl-2- methylamino-4-(3-pyridylmethyl)benzothiazole glucuronide. *J. Pharmacol. Exp. Ther.* **282**:866–872 (1997).
21. Y. Cui, J. König, J. K. Buchholz, H. Spring, I. Leier, and D. Keppler. Drug resistance and ATP-dependent conjugate transport mediated by the apical multidrug resistance protein, MRP2, permanently expressed in human and canine cells. *Mol. Pharmacol.* **55**:929–937 (1999).
22. H. Zeng, G. Liu, P. A. Rea, and G. D. Kruh. Transport of amphipathic anions by human multidrug resistance protein 3. *Cancer Res.* **60**:4779–4784 (2000).
23. E. Bakos, R. Evers, E. Sinko, A. Varadi, P. Borst, and B. Sarkadi. Interactions of the human multidrug resistance proteins MRP1 and MRP2 with organic anions. *Mol. Pharmacol.* **57**:760–768 (2000).
24. S. Dey, P. Hafkemeyer, I. Pastan, and M. M. Gottesman. A single amino acid residue contributes to distinct mechanisms of inhibition of the human multidrug transporter by stereoisomers of the dopamine receptor antagonist flupentixol. *Biochemistry* **38**:6630–6639 (1999).
25. A. L. Craddock, M. W. Love, R. W. Daniel, L. C. Kirby, H. C. Walters, M. H. Wong, and P. A. Dawson. Expression and transport properties of the human ileal and renal sodium- dependent bile acid transporter. *Am. J. Physiol.* **274**:G157–G169 (1998).
26. C. C. Martin and C. D. William. In I. M. Arias, J. L. Boyer, N. Fausto, W. B. Jakoby, D. A. Schachter, D. A. Shafrutz (eds.), *Liver: Biology and Pathobiology,* Raven Press, New York, 1994 pp. 719–767.
27. Y. Siow, A. Schurr, and G. C. Vitale. Diabetes-induced bile acid composition changes in rat bile determined by high performance liquid chromatography. *Life Sci.* **49**:1301–1308 (1991).